Acta Cryst. (1988). B44, 156–163

Structure and Steric Hindrance Analyses to Determine the Dynamical Disorder in 1-Iodoadamantane ($C_{10}H_{15}I$)

BY M. FOULON AND C. GORS

Laboratoire de Dynamique des Cristaux Moléculaires (UA 801 CNRS), Université de Lille I, 59655 Villeneuve d'Ascq CEDEX, France

(*Received* 4 *December* 1986; *accepted* 9 *October* 1987)

Abstract

A structure determination was undertaken to obtain a precise description of the disorder in the high-temperature phase of 1-iodoadamantane at 295 and 256 K. The compound crystallizes in the orthorhombic system (space group *Pmmn*) with $Z = 2$ [parameters at $T = 256$ K: $a = 8{\cdot}640$ (17), $b = 6{\cdot}693$ (13), $c = 8{\cdot}854$ (17) Å, $V = 512{\cdot}0$ Å^3, $D_x = 1{\cdot}70$ g cm^{-3}, λ(Mo $K\alpha$) = 0·7107 Å, $\mu = 31{\cdot}05$ cm^{-1}, $F(000) = 256$, $R = 3{\cdot}54$, $wR = 3{\cdot}75\%$ for 1211 observed reflections ($F_{obs} > 6\sigma_F$)]. The crystal was grown from a solution in methanol. The best refinements were obtained with either independent atoms or a rigid group in a Frenkel-model framework ($R \simeq 4\%$). These two models led to similar results but did not settle definitively the number and location of the molecular equilibrium positions. The relatively high values of the **TLS** components compared with those found for other adamantane derivatives are typical of a dynamical disorder corresponding to uniaxial molecular jumps. A steric hindrance analysis showed unambiguously that the molecule occupies two discernible equilibrium positions, the molecular mirror lying on the (010) crystal one. The two equilibrium positions are related to each other by a rotation of 60° around the C_3 molecular axis. The antiparallel arrangement of the molecular dipole axis leads to an antiferroelectric order in the distorted pseudocubic lattice, and may be compared with the local order in the glassy phase of 1-cyanoadamantane.

Introduction

This work is part of a systematic study of crystalline substituted adamantanes. Structure determination, NMR, IQNS and dielectric relaxation experiments lead to a better understanding of the properties of different phases: the molecular arrangement, dynamical disorder and phase transitions are strongly dependent on the substitution and electric dipole moment of the molecule.

1-Haloadamantanes (halo = F, Cl, Br) and 1-cyanoadamantane crystallize in a cubic plastic phase at room temperature or above and in (semi-) ordered phases at low temperature (Clark, McKnox, Mackle & McKervey, 1977). We report here on 1-iodoadamantane, which undergoes a first-order solid–solid transition at $T_t = 211$ K and melts at $T_m = 347$ K (Clark, McKnox, Mackle & McKervey, 1977).

Differential scanning calorimetry and studies on a polarizing microscope equipped with a heating stage have not revealed any plastic phase in 1-iodoadamantane (Cuvelier & Foulon, 1986). Partial structural results and NMR studies (Virlet, Quiroga, Boucher, Amoureux & Castelain, 1983) induced a model of quasi-free uniaxial rotation described by four discernible positions corresponding to 30° molecular jumps around the dipolar axis with an associated relaxation time $\tau_{m12} = 1{\cdot}7 \times 10^{-12}$ s at 295 K.

The low activation energy (5·1 kJ mol^{-1}), deduced from the Arrhenius law [$\tau_{m12} = 2{\cdot}1 \times 10^{-13} \exp(5{\cdot}1/RT)$], leads to the assumption of weak steric hindrance. In the present paper, we shall re-examine the orientational disorder and try to compare the structure of 1-iodoadamantane with those of other substituted adamantanes.

Experimental

The title compound was purified by successive sublimations and recrystallizations in methanol. Crystals were obtained by slow evaporation in methanol. Single crystals were sealed in a glass capillary to prevent sublimation and mounted on a Philips PW 1100 automatic diffractometer equipped with a nitrogen gas flow Nonius device.

Many of the crystals presented a growth twin in which the two individuals were related by a symmetry with respect to the ($\bar{1}10$) plane (Fig. 1*a*). The smaller individuals gave rise to extra Bragg reflexions in the reciprocal lattice of the larger ones (Fig. 1*b*). Measurement of the non-overlapping ones permitted evaluation of the relative volumes of the two individuals (5 and 95% respectively of the total crystal). Moreover, some of the extra Bragg reflexions can be indexed as ($h/2$, $k/2$, l) in the reciprocal lattice of the larger individual. This could have lead to an incorrect determination of the cell parameters and/or could have been interpreted as a superstructure in the local order.

0108-7681/88/020156-08$03.00

Reflexion intensities were collected at 295 and 256 K with the θ–2θ scan method. Crystal data and collection parameters are listed in Table 1. Unfortunately it was impossible to obtain the low-temperature phase on cooling on the diffractometer: the crystals break down at the transition temperature. It was, therefore, experimentally impossible to crystallize 1-iodoadamantane directly in its low-temperature phase ($T < 211$ K). In the high-temperature phase, the variation of crystal parameters with temperature has been measured (Fig. 2).

Lorentz–polarization and absorption corrections (*AGNOSTC*; Coppens, Leiserowitz & Rabinovich, 1965) were applied to the two sets of data ($0{\cdot}56 < k < 0{\cdot}62$).

Table 1. *Data-collection parameters*

	295 K	256 K
λ(Mo $K\bar{\alpha}$) (Å)	0·7107	0·7107
$(\sin\theta)/\lambda$ (Å^{-1})	0·049–0·766	0·049–0·807
h	0–13	0–13
k	0–10	0–10
l	0–13	0–13
No. of measured intensities	1813	1318
No. of independent intensities	1120	1276
No. of non-systematically absent intensities	1060	1211
No. of observed intensities $[F > 6\sigma(F)]$	560	672
Space group	*Pmmn*	*Pmmn*
a (Å)	8·676 (17)	8·640 (17)
b (Å)	6·703 (13)	6·693 (13)
c (Å)	8·860 (17)	8·854 (17)
Z	2	2
D_x (g cm^{-3})	1·69	1·70
μ (cm^{-1})	30·85	31·05
$F(000)$	256	256
No. of intensities for lattice parameter determination	25	25
Weights	$w = 1/[(\sigma_c^2 + 16 \times 10^{-4}F^2)^{1/2}]$	

Resolution

The systematic absences ($hk0$, $h+k = 2n$) indicate two possible space groups $P2_1mn$ and $Pmmn$ with $Z = 2$. For these two space groups, the Patterson method using the *SHELX* program (Sheldrick, 1976), shows that the I atom is located in the special positions (Wyckoff notation *a*) $[x_I,0,z_I$; $\frac{1}{2}+x_I,\frac{1}{2},\bar{z}]$ and $[0,0,z_I$; $\frac{1}{2},\frac{1}{2},\bar{z}_I]$, respectively.

A Fourier difference map located the C0 atom (for numbering see Fig. 3); the I–C0 bond (along the dipolar moment of the molecule) is on the **c** axis. The positions of the I and C0 atoms were confirmed by direct methods (*MULTAN*77; Main, Lessinger, Woolfson, Germain & Declercq, 1977). None of the remaining C atoms of the adamantyl group could be located precisely. The Fourier synthesis showed a residual electronic density distributed around the I–C0 dipolar axis, in agreement with the expected orientational disorder of the adamantyl group.

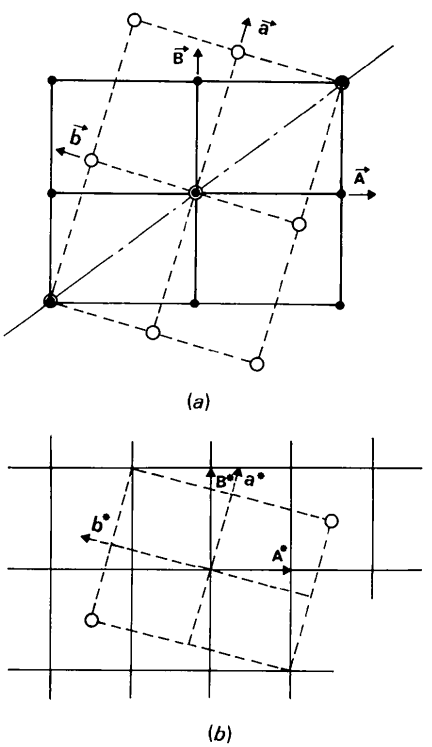

Fig. 1. (*a*) Direct-planes lattices **A**,**B** for the larger and **a**,**b** for the smaller crystal. (*b*) Reciprocal-planes lattices **A***,**B*** for the larger and **a***,**b*** for the smaller crystal.

Refinements

Several strategies were undertaken to establish unambiguously if the adamantyl group, rotating around

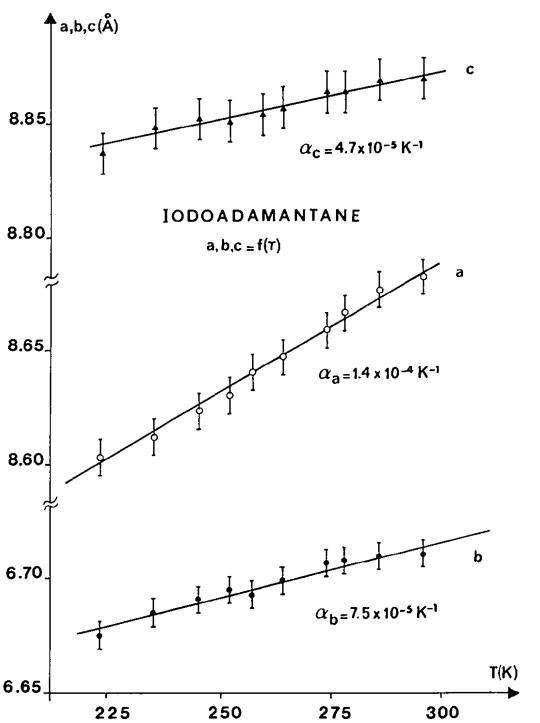

Fig. 2. Variation of cell parameters (Å) with temperature (K).

the I–C0 bond, occupies an infinity of equilibrium positions (cylindrical electronic density, CED) or some particular positions. According to the C_{3v} molecular and (*m* or *mm*) site symmetries (respective to $P2_1mn$ or *Pmmn*), some assumptions concerning the equilibrium positions have been made.

One of the molecular mirror planes may be in a general orientation or in a special one, *i.e.* on a crystal mirror plane [(010), (100), or (010)] or any combination of the two last positions. The five possibilities explored are depicted in Fig. 4 and lead to one, two or four molecular orientations. These are noted through the coordinates of the C1 atom ($\bar{x}0z$, $x0z$, $0\bar{y}z$, $0yz$). The schematic molecule is drawn by projection of the plane containing atoms C1, C2 and C3 in the (**a**,**b**) plane.

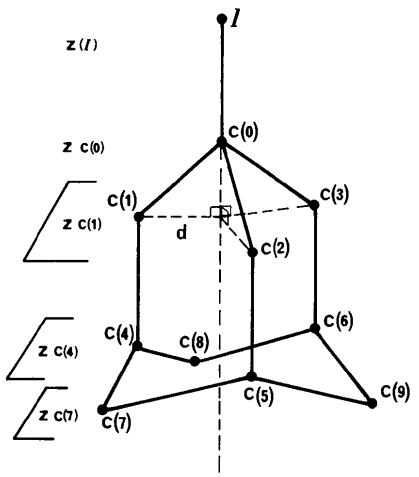

Fig. 3. Molecular geometry with numbering of atoms.

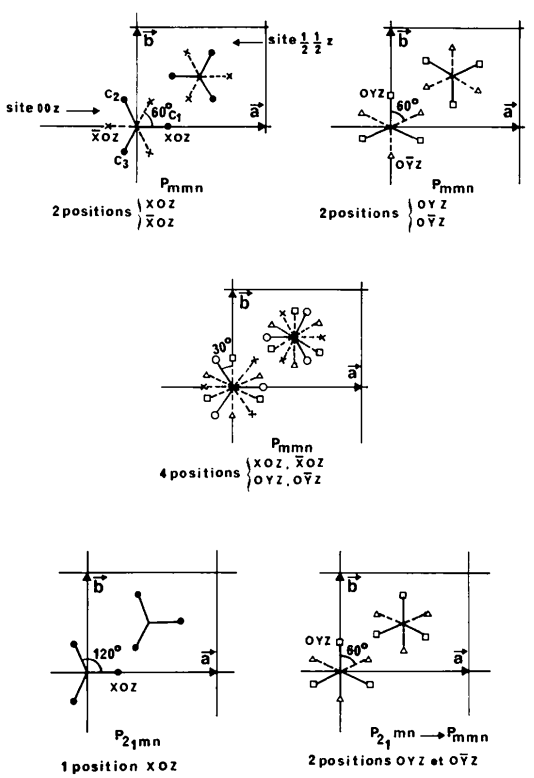

Fig. 4. Five possible molecular equilibrium positions.

The number of refined parameters was reduced by use of symmetry considerations. The coordinates of all the atoms were geometrically constrained by the C_{3v} molecular symmetry. The site symmetry places restrictions on the components of the temperature tensors. In a first stage, the atoms were refined independently with anisotropic temperature factors (*SHELX*76; Sheldrick, 1976). Six parameters described the heavy-atom coordinates: the distance *d* to the dipolar axis and the *z* coordinates [z_I, z_{C0}, $z_{C1,C2,C3}$, $z_{C4,C5,C6}$, $z_{C7,C8,C9}$] (Fig. 3). In a second stage, the molecule was introduced as a rigid group. The atom coordinates were those found by the previous refinements. The molecular vibration was described by the classical **T**, **L**, **S** tensors (Schomaker & Trueblood, 1968). The structure was refined according to either a CED or a Frenkel model (transformed version of *ORION*: André, Fourme & Renaud, 1971).

The first model states that the probability of the molecular orientation is constant around the **c** axis: this procedure was described in the study of the glassy phase of 1-cyanoadamantane (Foulon, Lefebvre, Amoureux, Muller & Magnier, 1985).

The second model assumes that the molecule occupies one, two or four equilibrium positions. According to the symmetry, only eight non-vanishing components of the **T**, **L**, **S** tensors describe the molecular thermal vibrations for the Frenkel model (T_{ii}, L_{ii}, S_{12} and S_{21}) (Schomaker & Trueblood, 1968). The L_{33} term must be set to 0·0 in the CED model.

Results

The results for the two experimental temperatures are summarized in Table 2 (for independent atoms) and Table 3 (for the rigid-body model) for the two possible space groups and the different orientations of the adamantyl group. For each set we give the site occupation, the space group, the *R* factors (*R*, *wR*), the number N_T of structure factors included in the refinement, and comments on the results. The maximum and minimum values of the residual electronic density, and the refined *d* distance described above, are also reported in Table 2. The components of the **T**, **L**, **S** tensors complete Table 3. In terms of convergence, most of the trials give comparable results. As is well known, the residual factors cannot be the only criterion for discerning the correct solution.

All the solutions with a molecule in a $0yz$ position were rejected since the refinement leads to abnormally

Table 2. *Results of the refinements with 'independent' atoms*

Positions of the molecule in 000 and $\frac{1}{2}\frac{1}{2}\frac{1}{2}$ sites	Space group	R (%)	wR (%)	N_T	$\rho_{max,min}$ (e Å^{-3})	d (Å)	Refinement procedure	Comments
(*a*) $T = 256$ K								
1 Iodine	*Pmmn*, $P2_1mn$	14·7	15·4	594	25·8, −7·2	—	A	
$x0z$ (000), $\bar{x}0z$ ($\frac{1}{2}\frac{1}{2}\frac{1}{2}$)	$P2_1/m$	6·8	7·5	675	2·4, −3·0	1·434	A, distinct positions for the two sites	AMG, d(C1−C4) = 1·74 Å
$x0z$	$P2_1mn$	4·1	4·4	672	3·4, −2·5	1·425	A, 1 orientation	HRED
$0yz$ ($\frac{1}{2}$), $0\bar{y}z$ ($\frac{1}{2}$)	*Pmmn*	5·4	6	672	3·5, −30	1·277	A, 2 orientations	AMG, HRED, DWF anomalies
xxz, $\bar{x}xz$, $x\bar{x}z$ ($\frac{1}{4}$)	*Pmmn*	5·5	6	672	3·6, −3·5	1·436	A, 4 general orientations	HRED, σ high
$x0z$, $\bar{x}0z$, $0yz$, $0\bar{y}z$ ($\frac{1}{4}$)	*Pmmn*	3·4	3·4	672	1·25, −2·4	1·409	A, 4 special orientations	AMG, DWF anomalies: (No. of parameters) × 2
$x0z$, $\bar{x}0z$ (0·95), $0yz$, $0\bar{y}z$ (0·05)	*Pmmn*	13·1	13·5	672	17·4, −8		A for $x0z$, I for $0yz$	Divergence
$x0z$, $\bar{x}0z$ ($\frac{1}{2}$)	*Pmmn*	3·5	3·8	672	1·3, −2·5	1·425	A	Correct solution (Δ/σ_{max} = 0·05)
(*b*) $T = 295$ K								
$0yz$, $0\bar{y}z$ ($\frac{1}{2}$)	*Pmmn*	5·8	6·2	560	4·2, −3·2	1·285	A	AMG, DWF anomalies
$x0z$, $\bar{x}0z$ ($\frac{1}{2}$)	*Pmmn*	4·6	4·7	560	1·9, −3·0	1·428	A	Correct solution (Δ/σ_{max} = 0·06)

Abbreviations: A = anisotropic Debye–Waller factors, I = isotropic Debye–Waller factors, HRED = high residual electronic density, DWF = Debye–Waller factors, AMG = anomalous molecular geometry.

Table 3. *Results of the refinements with the rigid-group model, space group Pmmn*

Positions in the 000 and $\frac{1}{2}\frac{1}{2}\frac{1}{2}$ sites	R (%)	wR (%)	$T_{11}^{1/2}$ (Å)	$T_{22}^{1/2}$ (Å)	$T_{33}^{1/2}$ (Å)	$L_{11}^{1/2}$ (°)	$L_{22}^{1/2}$ (°)	$L_{33}^{1/2}$ (°)	$S_{12} \times 10^{-4}$ (rad Å)	$S_{21} \times 10^{-4}$ (rad Å)	N_T	Model
(*a*) $T = 256$ K												
∞	5·8	10·0	0·219 (7)	0·250 (7)	0·186 (1)	4·9 (0·3)	3·9 (0·4)	0	−149 (7)	50 (7)	674	CED
$0yz$ $0\bar{y}z$	6·4	12·3	0·217 (10)	0·273 (10)	0·184 (2)	3·9 (0·6)	3·8 (0·5)	27·5 (1·5)	−114 (11)	49 (9)	674	Frenkel 2 positions
($x0z$–$\bar{x}0z$) $\frac{1}{2}$, ($0yz$–$0\bar{y}z$) $\frac{1}{2}$	6·5	6·7	0·232 (14)	0·262 (13)	0·182 (2)	3·9 (0·7)	2·6 (1·0)	11·5 (1·4)	−122 (15)	30 (14)	674	Frenkel 4 positions
$x0z$–$\bar{x}0z$	3·7	6·1	0·214 (4)	0·265 (4)	0·187 (1)	4·5 (0·2)	4·10 (0·2)	12·4 (0·3)	−124 (4)	55 (4)	674	Frenkel 2 positions
(*b*) $T = 295$ K												
∞	6·2	10·8	0·247 (9)	0·279 (7)	0·199 (1)	5·1 (0·3)	4·3 (0·5)	0	−175 (80)	52 (9)	557	CED
$0yz$ $0\bar{y}z$	7·8	14·6	0·255 (12)	0·285 (10)	0·198 (2)	4·9 (0·5)	4·0 (0·7)	25·7 (1·4)	−159 (11)	40 (13)	557	Frenkel 2 positions
($x0z$–$\bar{x}0z$) $\frac{1}{2}$, ($0yz$–$0\bar{y}z$) $\frac{1}{2}$	6·3	10·9	0·243 (8)	0·280 (7)	0·199 (1)	5·1 (0·3)	4·6 (0·4)	8·4 (2·1)	−173 (8)	57 (8)	557	Frenkel 4 positions
$x0z$ $\bar{x}0z$	4·5	7·5	0·238 (5)	0·289 (4)	0·199 (1)	5·0 (0·2)	4·6 (0·3)	13·1 (0·4)	−154 (5)	64 (5)	557	Frenkel 2 positions

large temperature factors or absurd molecular geometry. A more satisfactory result is obtained in the *Pmmn* space group with two equally probable molecules in each site with an orientation $x0z$ and $\bar{x}0z$ of the adamantyl group, leading to a 60° molecular jump [coincidence of the molecular symmetry and (010) lattice planes]. The CED model must be considered as intermediate between these two possibilities.

The problem of distinguishing the correct solution arises from the low contribution of the adamantyl group to the structure factors. The first refinement with only the I atom gave a relatively low R factor (0·15).

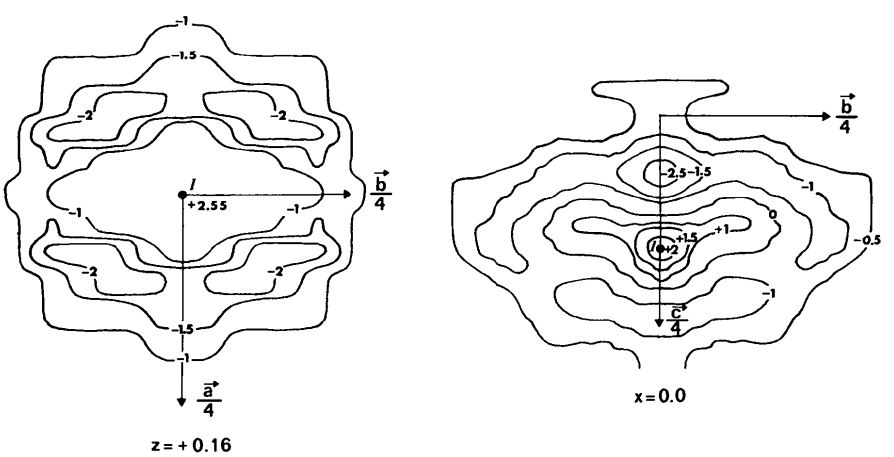

Fig. 5. Anomalous residual electronic density (e Å^{-3}) in the vicinity of the I atom.

Subtracting the I and C0 contributions to the structure factors, it is possible to select those (F_{ADA}) showing sensitivity to the adamantyl group. In a final stage, we confirmed the chosen solution, by a refinement including only those 76 selected ($F_{ADA} \geq F_{obs}/5$) structure factors (about 10% of those used in the previous refinements). The refinement converges, for the $x0z$, $\bar{x}0z$ model ($R = 5\%$), but diverges for the $0yz$, $0\bar{y}z$ one ($R \rightarrow 32\%$).

Residual electronic density

The final Fourier difference map (Fig. 5) shows some anomalous residual electronic density around the I atom: a positive density on the C0–I bond ($\rho_{max} = 2{\cdot}5$ e Å^{-3}) and an important negative one, well defined around the dipolar axis at about 1·2 Å from it ($\rho_{min} = -2{\cdot}5$ e Å^{-3}). These anomalies may be due to the unrealistic spherical approximation for the scattering factors of the I atom which might be considered as anisotropic.

Discussion

Comments are developed on the structure at $T = 256$ K but may be transposed at $T = 295$ K. The two molecules in each site are related by $x\bar{y}z$ symmetry. The final atomic parameters of the so-called $x0z$ orientation are listed in Table 4.*

(*a*) *The Frenkel model*

A C atom of the adamantyl group has six equivalent positions (symmetry $C_3 \times 2$ equilibrium positions). The rotational probability function $P(\varphi)$ for such an atom can be calculated using a Gaussian distribution:

$$P(\varphi) = [3/6(2\pi L_{33})^{1/2}] \sum_{i=1}^{6} \{\exp[-(\varphi-\varphi_0^i)^2/2L_{33}]\},$$

in which φ_0^i is the ith equilibrium angle value, and L_{33} is the square librational amplitude parallel to the dipolar axis.

$P(\varphi)$ is drawn in Fig. 6 for the three models: (i) cylindrical electronic density $P(\varphi) = 3/2\pi$, (ii) the Frenkel model for the two positions $x0z$ and $\bar{x}0z$, and (iii) the Frenkel model for the two positions $0yz$ and $0\bar{y}z$. This probability distribution confirms clearly the sixth-order rotation between two equilibrium positions. The previous model, supported by NMR experiments and partial crystallographic elements, and which proposed four equilibrium positions, seems to be ruled out. Nevertheless we can deduce the relaxation time $\tau_{m6} = 6{\cdot}3 \times 10^{-12}$ s at 295 K from the measured τ_{m12} (Virlet, Quiroga, Boucher, Amoureux & Castelain, 1983).

Table 4. *Atomic coordinates* ($\times 10^4$) *at* 256 K

$U_{eq} = \frac{1}{3}\sum_i\sum_j U_{ij} a_i^* a_j^* \mathbf{a}_i.\mathbf{a}_j$ ($\times 10^2$).

	x	y	z	U_{eq}(Å^2)
I	0 (1)	0 (1)	1565 (1)	73 (1)
C0	0 (1)	0 (1)	−927 (6)	43 (3)
C1	1649 (4)	0 (1)	−1441 (5)	77 (11)
C2	−828 (2)	−1849 (4)	−1441 (5)	61 (10)
C3	−828 (2)	1849 (4)	−1441 (5)	88 (10)
C4	1649 (4)	0 (1)	−3211 (7)	102 (18)
C5	−828 (2)	−1849 (4)	−3211 (7)	63 (11)
C6	−828 (2)	1849 (4)	−3211 (7)	83 (11)
C7	−1655 (4)	0 (1)	−3784 (7)	71 (13)
C8	823 (2)	1843 (4)	−3784 (7)	86 (15)
C9	823 (2)	−1843 (4)	−3784 (7)	116 (15)

(*b*) *Molecular geometry*

Intramolecular distances and angles are given in Table 5 and are in agreement with previous results for such molecules.

The important libration of the molecule around the dipolar axis explains the shortening of the distance d (1·423 Å). To a first approximation, a correction ($\Delta d = 0{\cdot}5 \times d \times L_{33}$) (Cruickshank, 1956) gives a d value of 1·459 Å close to the expected value (1·453 Å).

The length (1·567 Å) of the C1–C4 bond (and its equivalent) deviates slightly from its expected 'chemical' value (1·54 Å) but the R factor is not significantly affected by constraining the bond to this value. (This bond suffers only minor shortening due to libration effects.) The small number of F factors sensitive to the adamantyl group (*i.e.* the uniaxial disorder) explains this anomaly.

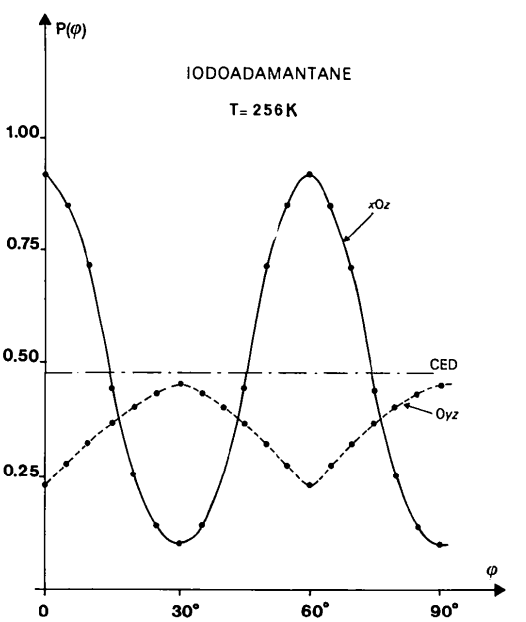

Fig. 6. Orientational probability function for a C atom according to three different models.

*A list of structure factors has been deposited with the British Library Document Supply Centre as Supplementary Publication No. SUP 44478 (5 pp.). Copies may be obtained through The Executive Secretary, International Union of Crystallography, 5 Abbey Square, Chester CH1 2HU, England.

Table 5. *Intramolecular distances* (Å) *and angles* (°)

I–C0	2·207 (5)	C4–C8	1·513 (4)
C0–C1	1·496 (4)	C4–C9	1·513 (4)
C0–C2	1·500 (3)	C5–C7	1·516 (4)
C0–C3	1·500 (3)	C5–C9	1·514 (4)
C1–C4	1·567 (8)	C6–C7	1·516 (4)
C2–C5	1·567 (8)	C6–C8	1·514 (4)
C3–C6	1·567 (8)		

I–C0–C1	107·7 (2)	C8–C4–C9	109·3 (3)
I–C0–C2	107·7 (2)	C2–C5–C7	109·5 (3)
I–C0–C3	107·7 (2)	C2–C5–C9	109·6 (3)
C1–C0–C2	111·2 (3)	C7–C5–C9	109·2 (3)
C1–C0–C3	111·2 (3)	C3–C6–C7	109·5 (3)
C2–C0–C3	111·2 (3)	C3–C6–C8	109·6 (3)
C0–C1–C4	107·7 (3)	C7–C6–C8	109·2 (3)
C0–C2–C5	107·7 (3)	C5–C7–C6	109·4 (3)
C0–C3–C6	107·7 (3)	C4–C8–C6	109·5 (3)
C1–C4–C8	109·6 (3)	C4–C9–C5	109·5 (3)
C1–C4–C9	109·6 (3)		

(*c*) *Thermal motion*

The U_{ij} refined by anisotropic independent atoms or calculated from the **T**, **L**, **S**, tensors are nearly similar. The translation **T** tensor shows a large anisotropy ($T_{22} = 1{\cdot}53T_{11}$) which excludes C_3 symmetry ($T_{11} = T_{22}$).

The large L_{33} term ($L_{33}^{1/2} = 12{\cdot}4°$) results from the orientational uniaxial disorder around the dipolar axis. The L_{11} and L_{22} values ($L_{11}^{1/2} = 4{\cdot}5°$ and $L_{22}^{1/2} = 4{\cdot}1°$), which measure the librations perpendicular to the dipolar axis, seem too large for a non-plastic phase; in the plastic phases of 1-cyano- and 1-chloroadamantane characterized by the tumbling of the molecule, the corresponding values are 3 and 7° respectively (Foulon, Lefebvre, Amoureux, Muller & Magnier, 1985; Magnier, 1986).

The principal axes of **T** and **L** evidently coincide with the **a**,**b**,**c** lattice vectors.

The fractional coordinates of the centre of reaction are simply calculated by $\rho_x^0 = 0$, $\rho_y^0 = 0$, $\rho_z^0 = (S_{12} - S_{21})(L_{11} + L_{22}) = -0{\cdot}180$. The centre of reaction is situated between the I atom and the adamantyl-group mass centre G (0,0, $\simeq -\frac{1}{4}$), at 0·74 Å from it.

Molecular packing and steric hindrance

(*a*) *Molecular arrangement*

The intermolecular distances between the six nearest-neighbouring I atoms are much greater than the sum of the van der Waals radii (6·119 and 6·693 Å).

The molecular packing is shown schematically in Figs. 7(*a*) and 7(*b*) where the molecular solid shape is obtained assuming spheres of van der Waals radii for constituent atoms. The structure may be described by a succession of planes spaced at $z/c = \frac{1}{2}$ from each other. The content of a plane at $z/c = 0$ is drawn in Fig. 7(*a*).

The dipolar axis is always perpendicular to the (**a**,**b**) plane but in an antiparallel manner in two successive planes. Fig. 7(*b*) shows the molecules whose mass centres and dipolar axes belong to plane ($\mathbf{A}_c$, **c**) with $\mathbf{A}_c = \mathbf{a}+\mathbf{b}$. This dipolar arrangement leads to an antiferroelectric order similar to that evidenced locally in the glassy phase of 1-cyanoadamantane (Foulon, Lefebvre, Amoureux, Muller & Magnier, 1985; Descamps, Caucheteux, Odou & Sauvajol, 1984; Lefebvre, Rolland, Sauvajol & Hennion, 1985; Bee, Foulon, Amoureux, Caucheteux & Poinsignon, 1987).

(*b*) *Lack of plastic phase*

In order to explain the lack of a plastic phase in 1-iodoadamantane, it is of interest to build a pseudo-cubic lattice from the actual orthorhombic one.

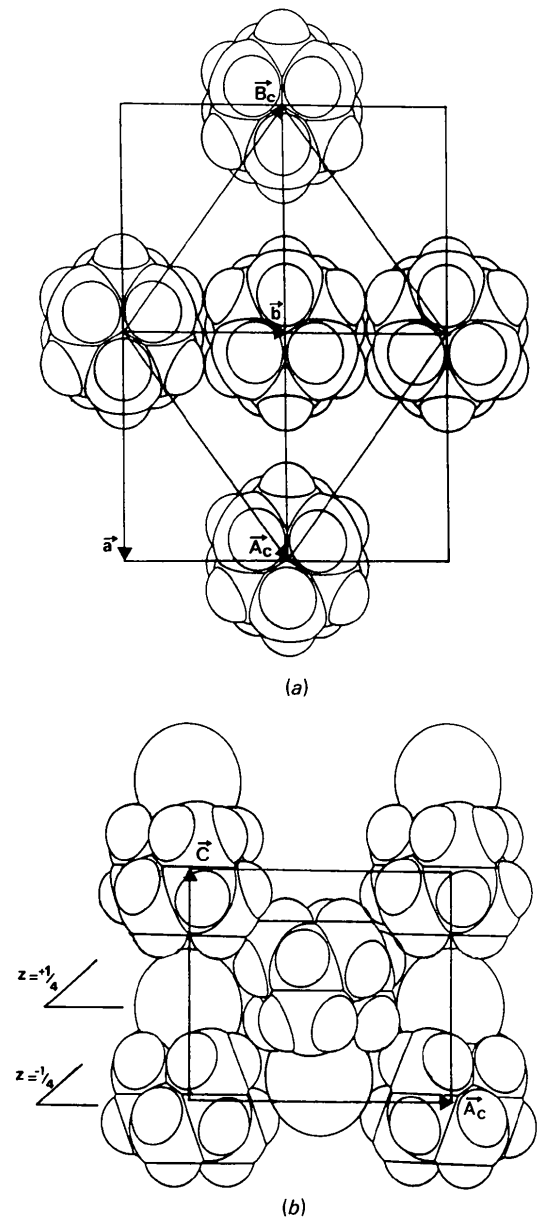

Fig. 7. (*a*) Content of the (**a**,**b**) plane [molecular mass centres belong to (**a**,**b**)]. (*b*) Content of the ($\mathbf{A}_c$,**C**) plane [molecular mass centres belong to ($\mathbf{A}_c$,C)].

The lattice built on the adamantyl mass centres (denoted G) of neighbouring molecules describes a strongly distorted pseudo-face-centred cubic lattice according to the following transformations ($\mathbf{A}_c$, $\mathbf{B}_c$, $\mathbf{C}_c$ = pseudo-cubic lattice vectors; **a**,**b**,**c** = actual orthorhombic vectors):

$$\mathbf{A}_c = \mathbf{a} + \mathbf{b}; \quad \mathbf{B}_c = \mathbf{b} - \mathbf{a}; \quad \mathbf{C}_c = \mathbf{c}.$$

At 256 K:

$|\mathbf{A}_c| = |\mathbf{B}_c| = 10{\cdot}93$ Å, $|\mathbf{C}_c| = 8{\cdot}854$ Å, $\angle A_c - B_c = 104{\cdot}5°$.

At 295 K:

$|\mathbf{A}_c| = |\mathbf{B}_c| = 10{\cdot}96$ Å, $|\mathbf{C}_c| = 8{\cdot}859$ Å, $\angle A_c - B_c = 104{\cdot}6°$.

A similar study for 1-cyanoadamantane in the low-temperature phase (Foulon, Amoureux, Sauvajol, Cavrot & Muller, 1984) showed that this so-built pseudo-cubic lattice tends to the cubic lattice of the plastic phase with increasing temperature.

In contrast, for 1-iodoamantane the development of pseudo-cubic parameters increases the distortion: a plastic phase, similar to those of the other 1-substituted adamantanes, cannot be expected.

Some geometrical and energy considerations relating to the essential difference between 1-iodoadamantane and other substituted adamantanes, the lack of plastic phase, are discussed below.

(i) *Molecular shape.* Substitution of a heavy I atom for an H atom of adamantane leads to a molecular shape rather different from the so-called globular one. This cannot be the predominant feature as the shape of 1-cyanoadamantane is very similar to that of 1-iodoadamantane, and crystallizes in a plastic phase over $T = 283$ K.

(ii) *Inertial moment.* The inertial moments parallel and perpendicular ($J_{\parallel}$, $J_{\perp}$) to the dipolar axis are very different. Furthermore the $J_{\perp}$ inertial moment is much greater than for other substituted adamantanes: 583, 593, 896, 1210 a.m.u. Å^2 for the CN, Cl, Br, I derivatives, calculated with respect to the centre of mass of the adamantyl group. In these derivatives, the orientational disorder occurring in the plastic phase is characterized by molecular tumbling, around an axis perpendicular to the dipolar one.

For 1-iodoamantane, the energy barrier for such a reorientation should be so high that translational disorder (melting) occurs before orientational disorder.

(iii) *Atom–atom interaction.* The I–I interaction is a puzzling and not yet resolved problem. A charge-transfer effect may explain the stability of the orthorhombic semi-ordered phase, but cannot be measured quantitatively. The anomalous residual electronic density in the vicinity of the I atom might be related to this charge-transfer effect.

(c) *Steric hindrance*

A first approach to studying the steric hindrance is to compare the interatomic distances of neighbouring molecules with the sum of the corresponding atomic van der Waals radii. The computation was limited to one molecule denoted G_0 surrounded by its 10 nearest neighbours (G_1 to G_{10} in Figs. 8*a* and 8*b*). The I and H atoms, replaced to their 'chemical' positions (d_{CH} = 1·08 Å and H–C–H = 109°) were considered. Neighbouring I atoms do not hinder the rotation of the origin molecule G_0 ($d_{I-H_{min}} = 3{\cdot}38$ Å).

To generate all the 4^{11} possible local configurations, the 11 molecules are introduced in the four positions described in the structure refinement (denoted $x0z$, $\bar{x}0z$, $0yz$, $0\bar{y}z$). One configuration is arbitrarily rejected if the intermolecular H–H distance between G_0 and one of its neighbours is lower than 2·2 Å (van der Waals radii sum 2·40 Å). According to this condition, the molecules G_3,G_4,G_5,G_6, in any positions, do not 'interact' with G_0.

Among the 4^7 remaining configurations to be examined, 4680 agree with the choosen criterion. Only 72 of them involve positions $0yz$ or $0\bar{y}z$ of the origin molecule. This conclusion makes these two molecular orientations highly improbable and confirms unambiguously the structural analysis. Moreover, when the

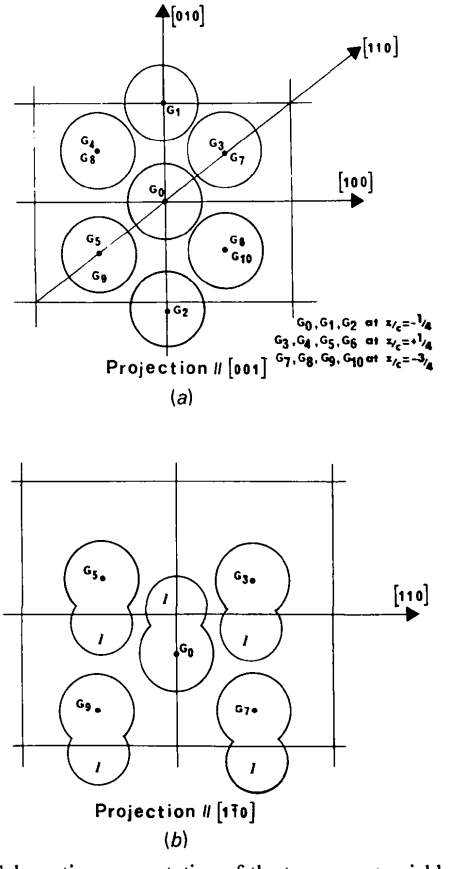

Fig. 8. Schematic representation of the ten nearest neighbours of a molecule (denoted G_0).

ten neighbouring molecules are placed in the $x0z$ (or $\bar{x}0z$) orientation, the origin molecule can rotate, without hindrance, from the $x0z$ to the $\bar{x}0z$ equilibrium position (according to the previous criterion on the H—H distance). The high steric hindrance along the **b** axis explains the low contraction of the **b** parameter with temperature, compared with that along **a** (Fig. 2).

Concluding remarks

By careful refinements, probability distributions and steric hindrance considerations we have proved that the orientational disorder of 1-iodoadamantane can be described with a Frenkel model. The rotation between the two equilibrium positions is quasi-free.

An antiferroelectric order has been pointed out similar to that locally encountered in the glassy phase of 1-cyanoadamantane. Some geometrical and energy features have been qualitatively examined to explain the lack of plastic phase in comparison to other adamantane derivatives.

An extension of this study will be to investigate the behaviour of mixtures of 1-cyano- and 1-iodoadamantane. If these two compounds syncrystallize, complete thermodynamic, structure and molecular-motion analyses should allow the part played by physical parameters in a glassy crystalline phase (*i.e.*, molecular geometry, dipolar interaction, slow molecular tumbling and particularly the local order) to be quantified.

The authors are grateful to M. Muller and D. Prevost for preparing the sample.

References

ANDRÉ, D., FOURME, R. & RENAUD, M. (1971). *Acta Cryst.* B**27**, 2371–2380.
BEE, M., FOULON, M., AMOUREUX, J. P., CAUCHETEUX, C. & POINSIGNON, C. (1987). *J. Phys. C.* In the press.
CLARK, T., MCKNOX, O., MACKLE, H. & MCKERVEY, M. A. (1977). *J. Chem. Soc. Faraday. Trans.* **73**, 1224–1231.
COPPENS, P., LEISEROWITZ, L. & RABINOVICH, D. (1965). *Acta Cryst.* **18**, 1035–1038.
CRUICKSHANK, D. W. J. (1956). *Acta Cryst.* **9**, 757–758.
CUVELIER, P. & FOULON, M. (1986). Private communication.
DESCAMPS, M., CAUCHETEUX, C., ODOU, G. & SAUVAJOL, J. L. (1984). *J. Phys. Lett.* **45**, L719–727.
FOULON, M., AMOUREUX, J. P., SAUVAJOL, J. L., CAVROT, J. P. & MULLER, M. (1984). *J. Phys. C*, **17**, 4213–4229.
FOULON, M., LEFEBVRE, J., AMOUREUX, J. P., MULLER, M. & MAGNIER, D. (1985). *J. Phys. (Paris)*, **46**, 919–926.
LEFEBVRE, J., ROLLAND, J. P., SAUVAJOL, J. L. & HENNION, B. (1985). *J. Phys. C*, **18**, 241–255.
MAGNIER, D. (1986). Thesis, Univ. of Lille, France.
MAIN, P., LESSINGER, L., WOOLFSON, M. M., GERMAIN, G. & DECLERCQ, J.-P. (1977). *MULTAN77. A System of Computer Programs for the Automatic Solution of Crystal Structures from X-ray Diffraction Data.* Univs. of York, England, and Louvain, Belgium.
SCHOMAKER, V. & TRUEBLOOD, K. N. (1968). *Acta Cryst.* B**24**, 63–76.
SHELDRICK, G. M. (1976). *SHELX76.* Program for crystal structure determination. Univ. of Cambridge, England.
VIRLET, J., QUIROGA, L., BOUCHER, B., AMOUREUX, J. P. & CASTELAIN, M. (1983). *Mol. Phys.* **48**, 1289–1303.

Acta Cryst. (1988). B**44**, 163–172

Synchrotron X-ray Data Collection and Restrained Least-Squares Refinement of the Crystal Structure of Proteinase K at 1·5 Å Resolution

BY CH. BETZEL,* G. P. PAL AND W. SAENGER

Institut für Kristallographie, Freie Universität Berlin, Takustrasse 6, *D*-1000 *Berlin* 33, *Federal Republic of Germany*

(*Received* 2 *June* 1987; *accepted* 22 *September* 1987)

Abstract

The structure of the serine endopeptidase proteinase K (279 amino acid residues; 28 790 daltons) has been refined by restrained least-squares methods to a conventional R value of 16·7% employing synchrotron film data of 30 812 reflections greater than 3σ in the 5·0 to 1·5 Å resolution range. During refinement, the molecular structure was restrained to known stereochemistry, with root-mean-square (r.m.s.) deviation of 0·015 Å from ideal bond lengths. The average atomic temperature factor, B, is 11·1 Å^2 for all atoms. The final model comprises 2020 protein atoms and 174 solvent molecules (which were given unit occupancies). Four corrections to the amino acid sequence were made, which were confirmed later by sequence analysis of the proteinase K gene: a deletion of one glycine in position 80; a change of sequence in position 207–208 and insertions of the dipeptide 210–211 and of residue 270. The r.m.s. deviation in the α-C atomic positions between the final refined model and the initial model

* Present address: European Molecular Biology Laboratory, Hamburg Outstation, c/o DESY, Notkestrasse 85, D-2000 Hamburg 52, Federal Republic of Germany.

0108-7681/88/020163-10$03.00